

# Energy transfer to the phonons of a macromolecule through light pumping

Elham Faraji<sup>1,4,5</sup>, Roberto Franzosi<sup>2</sup>, Stefano Mancini<sup>1,3</sup>, and Marco Pettini<sup>4,5,\*</sup>

<sup>1</sup>School of Science and Technology, University of Camerino, I-62032 Camerino, Italy

<sup>2</sup>QSTAR and INO-CNR, largo Enrico Fermi 2, I-50125 Firenze, Italy

<sup>3</sup>INFN Sezione di Perugia, I-06123 Perugia, Italy

<sup>4</sup>Aix Marseille Univ, Université de Toulon, CNRS, CPT, Marseille, France

<sup>5</sup>CNRS Centre de Physique Théorique UMR7332, 13288 Marseille, France

\*marco.pettini@cpt.univ-mrs.fr

## ABSTRACT

In the present paper we address the problem of the energy downconversion of the light absorbed by a protein into its internal vibrational modes. We consider the case in which the light receptors are fluorophores either naturally co-expressed with the protein or artificially covalently bound to some of its amino acids. In a recent work [Phys. Rev. X 8, 031061 (2018)], it has been experimentally found that by shining a laser light on the fluorophores attached to a protein the energy fed to it can be channeled into the normal mode of lowest frequency of vibration thus making the subunits of the protein coherently oscillate. Even if the phonon condensation phenomenon has been theoretically explained, the first step - the energy transfer from electronic excitation into phonon excitation - has been left open. The present work is aimed at filling this gap.

## Introduction

The activation of out-of-equilibrium collective intramolecular vibrations of a model protein has been recently reported in Ref.<sup>1</sup>. This phenomenon has been induced by light pumping, realised by shining a laser light on an aqueous solution of BSA (Bovine Serum Albumin) protein molecules each one carrying a few fluorophores covalently attached to their Lysine residues. The fluorophores were excited with a blue light at 4880Å and then they re-emitted a broadband fluorescence radiation peaked at 5190Å, thus the difference between the absorbed and re-emitted photon energies resulted in a concentration of an average energy of 0.19 eV at the fluorophores sites which thus became "hot points" on each protein. A continuous energy supply of this kind was experimentally found effective to excite the vibrational modes of the proteins and, with an energy supply rate exceeding a suitable threshold, this eventually led to a phonon condensation phenomenon into the lowest vibrational frequency. The relevance of this out-of-equilibrium collective molecular vibrations consists in the possibility of activating long-range electrodynamic interactions between bio-macromolecules<sup>2</sup>. The reason is that, at thermal equilibrium, a macromolecule vibrates incoherently with a broad spectrum of modes, whereas the action of an external source of energy promoting a phenomenon of phonon condensation can induce the coherent motion of the molecular subunits, so that, the resulting collective vibration can bring about a large oscillating dipole moment. Under this condition long-range and resonant (thus selective) electrodynamic forces can be activated. In turn, these electrodynamic forces could help explaining the astonishing efficiency of the impressively complex biochemical machinery at work in living cells<sup>3</sup>, where the different actors (proteins, DNA and RNA) find their cognate partners and targets in the right place, at the right time and in the right sequence in an overcrowded environment (the cytosol). Electrodynamic resonant/selective forces are the

only possible one to act at a long distance, all the others (chemical bonds, Van der Waals and electrostatic forces) are in fact either intrinsically acting at very short distances, or are screened by the freely moving small ions in the cytosol. Actually, this is a longstanding theoretical scenario<sup>4-6</sup> which, for several reasons, has been discarded. However, the upgrade of Fröhlich's theoretical proposition in<sup>1,2</sup> and the experimental outcomes reported in<sup>1</sup>, represent a first crucial leap forward to ascertain whether the above mentioned hypotheses can be given experimental confirmation or refutation that can be attempted with the nowadays available technology<sup>7,8</sup>.

The Wu-Austin Hamiltonian from which Fröhlich rate equations can be derived by resorting to time dependent perturbation theory<sup>12</sup> reads as

$$\begin{aligned} \widehat{H}_{Tot} = & \sum_{\omega_i} \hbar \omega_i a_{\omega_i} \widehat{a}_{\omega_i} + \sum_{\Omega_j} \hbar \Omega_j b_{\Omega_j} \widehat{b}_{\Omega_j} + \sum_{\Omega'_k} \hbar \Omega'_k c_{\Omega'_k} \widehat{c}_{\Omega'_k} \\ & + \sum_{\omega_i, \Omega_j} \eta_{\omega_i \Omega_j} a_{\omega_i} \widehat{b}_{\Omega_j} + \sum_{\omega_i, \Omega'_k} \xi_{\omega_i \Omega'_k} a_{\omega_i} \widehat{c}_{\Omega'_k} + \sum_{\omega_{A_i}, \omega_{A_j}, \Omega_k} \chi_{\omega_i \omega_j \Omega_k} a_{\omega_i} \widehat{a}_{\omega_j} b_{\Omega_k} + \text{h.c.} \end{aligned} \quad (1)$$

where  $a_{\omega_i}, \widehat{a}_{\omega_i}$  are the quantum creation/annihilation operators for the vibrational normal modes of a biomolecule with frequency  $\omega_i$ . A thermal bath at temperature  $T_B$  toward which the normal modes of the biomolecule dissipate energy is represented by a collection of harmonic oscillators with characteristic frequencies  $\Omega_j$  whose annihilation/creation operators are  $\widehat{b}_{\Omega_j}$  and  $b_{\Omega_j}$ . In order to put the biomolecule out of thermal equilibrium, the external energy pumping is modeled by another thermal bath at a temperature  $T_S \gg T_B$  represented by a collection of harmonic oscillators with frequencies  $\Omega'_k$ , the quantum annihilation/creation operators of which are  $\widehat{c}_{\Omega'_k}$  and  $c_{\Omega'_k}$ . Then, besides linear interactions among the thermal baths modes and the biomolecule modes, mode-mode interactions among the biomolecule normal modes are considered to be mediated by the modes of the former thermal bath.

The aim of the present paper is to understand, qualitatively and quantitatively, how this model can be improved to better represent the experimental conditions realised in Ref.<sup>1</sup> for what specifically concerns the high temperature heat bath (at  $T_B$ ). In other words, how can we better describe the process of conversion of the photon energy received through electronic excitation of the fluorophores attached to a biomolecule (protein) into vibrational energy of the chain of subunits (amino acids) composing it. In what follows, we will tackle a simplified model with respect to that described by Eq.(1) by focusing on the energy transfer process from the light excited electrons of the fluorophores to the phonons of a chain of particles representing a chain of amino-acids, so this is intended as a first step toward an upgrade of the model in Eq.(1).

As we shall see, it is found that only a fraction of the initially available electron energy is released to the phonons of a biomolecule. Even an approximate estimate of this energy transfer process is very important for a better assessment of the physical conditions which are necessary to activate the intramolecular collective vibrations.

## Definition of the model

In Ref.<sup>1</sup> the external source of energy driving the phonon condensation was modeled (by one of us among the others) as high temperature heat bath. This was done to reformulate in a classical framework the Wu-Austin<sup>12</sup> quantum model leading to the original Fröhlich rate equations of Ref.<sup>4</sup>.

We now aim at refining this part of the model in view of a better understanding of the basic excitation mechanism that can bring a macromolecule out of thermal equilibrium.

In both cases of photo-excitation and, presumably, of ionic collisions, the excitation mechanism is supposed to be mediated by the molecular electron cloud. Therefore, the model describing the phenomenon that we want to investigate is borrowed from the standard Davydov and Holstein-Fröhlich models<sup>14-16</sup> to account for electron-phonon interaction. Hence, the following energy operator is assumed

$$\hat{H} = \hat{H}_{el} + \hat{H}_{ph} + \hat{H}_{int}, \quad (2)$$

where the first term  $\hat{H}_{el}$  is the electron energy operator

$$\hat{H}_{el} = \sum_{n=1}^N \left[ E_0 \hat{B}_n^\dagger \hat{B}_n + \epsilon \langle \hat{B}_n^\dagger \hat{B}_n \rangle \hat{B}_n^\dagger \hat{B}_n + J(\hat{B}_n^\dagger \hat{B}_{n+1} + \hat{B}_n^\dagger \hat{B}_{n-1}) \right], \quad (3)$$

with  $\hat{B}_n$  and  $\hat{B}_n^\dagger$  the annihilation and creation operators for the electron at any site  $n$  ( $n = 1, 2, \dots, N$ ) which labels the amino acid along the protein. The term  $E_0 \hat{B}_n^\dagger \hat{B}_n$  accounts for the initial "bare" electron energy distributed on several lattice sites according to initial shape of the electron wavefunction. The constant  $J$  is the nearest neighbour coupling energy of the electron tunnelling across two neighbouring amino acids, and  $\epsilon$  is the energy scale of the nonlinear electron-electron coupling. In this model we have considered only a longitudinal chain of amino acids. The moving electron - yielded by the excited fluorophore - interacts on its way with almost free electrons in each amino acid, and it may just propagate along the chain of amino-acids or make a disturbance which will allow a next electron to continue on the trip. Anyway, due to electron indistinguishability, the net effect is a traveling electron along the chain of amino-acids rather than an excitonic transfer because in this latter case there is no moving mass along the chain. Then the term  $\epsilon \langle \hat{B}_n^\dagger \hat{B}_n \rangle \hat{B}_n^\dagger \hat{B}_n$  has been introduced to take into account non-linear effects due to the interaction between the electron in motion along the chain and the electrons of the substrate of amino acids. In particular, the term takes into account effects related to the Coulombic repulsion between the traveling electron and the charges localized on the amino acids. The averaging is intended as the expectation value of  $\hat{B}_n^\dagger \hat{B}_n$  on the dynamically evolving state of the system.

The second term  $\hat{H}_{ph}$  in (2) is the phonon energy operator

$$\hat{H}_{ph} = \frac{1}{2} \sum_n \left[ \frac{\hat{p}_n^2}{M} + \Omega(\hat{u}_{n+1} - \hat{u}_n)^2 + \frac{1}{2} \mu(\hat{u}_{n+1} - \hat{u}_n)^4 \right], \quad (4)$$

where  $\hat{p}_n$  and  $\hat{u}_n$  are momentum and position operators for longitudinal displacements of amino acids at site  $n$ , respectively. Furthermore,  $M$  and  $\Omega$  are average values of the mass of the amino acids of a protein and of the spring constants of two neighbouring amino acids, respectively. The quartic term is a correction stemming from the power series which gives the harmonic term at the lowest order expansion around the minimum of interparticle interaction potential (typically nonlinear, as is the case, for example, of the Van der Waals potential). This term is responsible for phonon-phonon interaction, absent in the harmonic approximation; the parameter  $\mu$  sets the strength of the phonon-phonon coupling.

Finally, the third term  $\hat{H}_{int}$  in (2) is the electron-phonon interaction operator

$$\hat{H}_{int} = \sum_n \chi(\hat{u}_{n+1} - \hat{u}_n) \hat{B}_n^\dagger \hat{B}_n, \quad (5)$$

where  $\chi$  is the energy coupling parameter.

## Derivation of the dynamical equations with TDVP

In order to derive from the model Hamiltonian (2) the corresponding dynamical equations, we make a simplifying ansatz about the state vectors by assuming the following factorization

$$|\psi\rangle = |\Psi\rangle|\Phi\rangle \quad (6)$$

in which  $|\Psi\rangle$  describes an electron given a single quantum excitation and supposed to be free to propagate along the chain of  $N$  amino acids composing a protein

$$|\Psi(t)\rangle = \sum_n C_n(t) \hat{B}_n^\dagger |0\rangle_{el}, \quad (7)$$

where  $|0\rangle_{el}$  is the vacuum state of the Amide-I oscillators, and

$$|\Phi(t)\rangle = e^{-\frac{i}{\hbar} \sum [\beta_n(t) \hat{p}_n - \pi_n(t) \hat{u}_n]} |0\rangle_{ph}. \quad (8)$$

We then set

$$\begin{aligned} \langle \Phi | \hat{u}_n | \Phi \rangle &= \beta_n(t), \\ \langle \Phi | \hat{p}_n | \Phi \rangle &= \pi_n(t), \end{aligned} \quad (9)$$

where  $\beta_n(t)$  and  $\pi_n(t)$  are the average values of the longitudinal displacement and momentum of an amino acid, respectively.

To derive dynamical equation we now resort to the time-dependent variational principle (TDVP) in quantum mechanics. TDVP is a formulation of the time-dependent Schrödinger equation through variation of an action functional. The Schrödinger equation is obtained by requiring that the action functional be stationary under free variation of the time-dependent state. According to this principle, we define a new wave function  $|\phi\rangle$  in terms of  $|\psi\rangle$  in Eq. (6) as

$$|\phi(t)\rangle = e^{iS(t)/\hbar} |\psi(t)\rangle, \quad (10)$$

where  $S(t)$  is a time-dependent phase factor ( $S(t) \in \mathbb{R}$ ), which will be determined in a self-consistent manner and the normalization condition is  $\langle \phi | \phi \rangle = 1$ . The wave function  $|\phi\rangle$  satisfies the Schrödinger equation

$$i\hbar \langle \phi(t) | \partial_t | \phi(t) \rangle = \langle \phi(t) | \hat{H} | \phi(t) \rangle, \quad (11)$$

which according to Eq. (10) becomes

$$-\dot{S}(t) + i\hbar \langle \psi(t) | \partial_t | \psi(t) \rangle = \langle \psi(t) | \hat{H} | \psi(t) \rangle. \quad (12)$$

Integrating, we obtain

$$S(t) = \int_0^t \left[ i\hbar \langle \psi(t) | \partial_t | \psi(t) \rangle - \langle \psi(t) | \hat{H} | \psi(t) \rangle \right] dt. \quad (13)$$

We can now derive the equations of motion by requiring that the action with the Lagrangian

$$L = i\hbar \langle \psi(t) | \partial_t | \psi(t) \rangle - \langle \psi(t) | \hat{H} | \psi(t) \rangle, \quad (14)$$

to be stationary

$$\delta S(t) = \delta \int L dt = 0. \quad (15)$$

From Eqs. (6), (7), and (8) we write

$$\partial_t|\psi\rangle = (\partial_t|\Psi\rangle)|\Phi\rangle + |\Psi\rangle(\partial_t|\Phi\rangle), \quad (16)$$

and then arrive at

$$\langle\psi|\partial_t|\psi\rangle = \sum_n \left[ \dot{C}_n(t)C_n^*(t) + \frac{i}{2\hbar} \left( \dot{\pi}_n(t)\beta_n(t) - \pi_n(t)\dot{\beta}_n(t) \right) \right]. \quad (17)$$

Thus the Lagrangian (14) becomes

$$L = \sum_n \left\{ i\hbar\dot{C}_n(t)C_n^*(t) + \frac{1}{2} \left( \pi_n(t)\dot{\beta}_n(t) - \dot{\pi}_n(t)\beta_n(t) \right) - H(C_n, C_n^*, \beta_n, \pi_n) \right\}, \quad (18)$$

where

$$H(C_n, C_n^*, \beta_n, \pi_n) = \langle\psi(t)|\hat{H}|\psi(t)\rangle. \quad (19)$$

Imposing the condition (15), we get

$$\begin{aligned} \delta S(t) = \sum_n & \left\{ i\hbar \left( -\dot{C}_n^*(t)\delta C_n(t) + \dot{C}_n(t)\delta C_n^*(t) \right) + \dot{\beta}_n(t)\delta\pi_n(t) - \dot{\pi}_n(t)\delta\beta_n(t) \right. \\ & \left. - (\partial_{C_n}H)\delta C_n - (\partial_{C_n^*}H)\delta C_n^* - (\partial_{\beta_n}H)\delta\beta_n - (\partial_{\pi_n}H)\delta\pi_n \right\} = 0, \end{aligned} \quad (20)$$

from which it results

$$\begin{aligned} i\hbar\dot{C}_n &= \partial_{C_n^*}H \\ \dot{\beta}_n &= \partial_{\pi_n}H \\ \dot{\pi}_n &= -\partial_{\beta_n}H. \end{aligned} \quad (21)$$

The expectation value of the Hamiltonian is

$$\begin{aligned} \langle\psi|\hat{H}|\psi\rangle = \sum_n & \left[ E_0|C_n|^2 + \epsilon|C_n|^4 + J(C_n^*C_{n+1} + C_{n+1}^*C_n) \right. \\ & + \frac{1}{2} \left( \frac{1}{M}\pi_n^2 + \Omega(\beta_{n+1} - \beta_n)^2 + \frac{1}{2}\mu(\beta_{n+1} - \beta_n)^4 \right) \\ & \left. + \chi(\beta_{n+1} - \beta_n)|C_n|^2 \right]. \end{aligned} \quad (22)$$

So, from Eq. (22) we have

$$\begin{aligned} i\hbar\dot{C}_n &= \left( E_0 + 2\epsilon|C_n|^2 + \chi(\beta_{n+1} - \beta_n) \right) C_n + J(C_{n+1} + C_{n-1}), \\ M\ddot{\beta}_n &= \Omega(\beta_{n+1} - 2\beta_n + \beta_{n-1}) + \chi \left( |C_n|^2 - |C_{n-1}|^2 \right) \\ &+ \mu \left( (\beta_{n+1} - \beta_n)^3 - (\beta_n - \beta_{n-1})^3 \right). \end{aligned} \quad (23)$$

## Definition of the physical parameters for numerical simulations

Let us see how to make a physically reasonable choice of the coupling parameters entering the Hamiltonian. We borrow from Ref.<sup>17,18</sup> the estimates of the interaction energy between an electron and each of all the 20 amino acids (reported in Table 1). The average value of these interaction energies is  $\langle \Delta E \rangle = 0.74$  eV with a dispersion  $\sigma_E = 0.47$  eV. As a first rough picture of an electron tunnelling across the sequence of amino acids constituting a protein we can consider the electron of energy  $E_0$  moving in a periodic sequence of square potential barriers of height  $V_0 = 0.74$  eV and of width  $a = 4.5\text{\AA}$ , the average distance between two nearest neighboring amino acids<sup>14</sup>. We can then weigh the electron displacement operators between neighbouring sites with the probability  $P(n \rightarrow n \pm 1)$  of tunnelling from one potential well to the nearest ones. This is achieved by computing the transmission coefficient

$$T = \left[ 1 + \frac{V_0^2 \sinh^2 \beta a}{4E_0(V_0 - E_0)} \right]^{-1} \quad (24)$$

where  $\beta = [2m_e(V_0 - E_0)/\hbar^2]^{1/2}$ . Moreover, the coefficient of the electron displacement term in the Hamiltonian has to be a characteristic energy scale of the process, thus a natural choice is to set  $J \propto \langle \Delta E \rangle T$ , then, assuming that an electron is initially excited at any given point of the chain of amino acids and that it has the same probability of moving to the left or to the right, we add a factor 1/2 so that finally we have  $J = \frac{1}{2} \langle \Delta E \rangle T$ . Now, assuming  $E_0 = 0.19$  eV as initial value of the electron energy, we find  $J = 0.0585$  eV, whereas assuming that only a fraction  $\delta \in [0, 1]$  of the maximum available energy is kept by the electron, for example for  $\delta = 0.5$ , we find  $J = 0.031$  eV. For what concerns the electron-phonon coupling constant  $\chi$ , we make a rough estimate of its value as  $\chi = \Delta E / \Delta x = \sigma_E / \Delta x = \sigma_E / a = 0.47 \text{ eV} / 4.5 \text{\AA} \simeq 100$  pN.

Amino acid	EIIP Ry	EIIP eV	Amino acid	EIIP Ry	EIIP eV
Leu	0.0000	0.0000	Tyr	0.0516	0.7017
Ile	0.0000	0.0000	Trp	0.0548	0.7452
Asn	0.0036	0.0489	Gln	0.0761	1.0349
Gly	0.0050	0.0680	Met	0.0823	1.1192
Val	0.0057	0.0775	Ser	0.0829	1.1274
Glu	0.0058	0.0788	Cys	0.0829	1.1274
Pro	0.0198	0.2692	Thr	0.0941	1.2797
His	0.0242	0.3291	Phe	0.0946	1.2865
Lys	0.0371	0.5045	Arg	0.0959	1.3042
Ala	0.0373	0.5072	Asp	0.1263	1.7176

**Table 1.** Electron-Ion interaction potential (EIIP) value for amino acids. From Ref.<sup>17</sup>.

In what follows, in dimensionless units, we have  $\chi' = 0.81$ , and  $J' = 5$  with  $\delta = 0.5$ , while  $J' = 9$  with  $\delta = 1$ .

By rescaling time and lengths as  $t = \omega^{-1} \tau$  and  $\beta_n = L b_n$ , respectively, where  $L = \sqrt{\hbar \omega^{-1} M^{-1}}$ ,

the following dimensionless dynamical equations are obtained

$$\begin{aligned}
i\frac{dC_n}{d\tau} &= \left[ \left( E' + 2\epsilon'|C_n|^2 + \chi'(b_{n+1} - b_n) \right) C_n + J'(C_{n+1} + C_{n-1}) \right], \\
\frac{d^2b_n}{d\tau^2} &= \Omega'(b_{n+1} - 2b_n + b_{n-1}) + \chi'(|C_n|^2 - |C_{n-1}|^2) \\
&+ \mu'[(b_{n+1} - b_n)^3 - (b_n - b_{n-1})^3],
\end{aligned} \tag{25}$$

and the dimensionless expression of the Hamiltonian is

$$\begin{aligned}
\langle \psi | \hat{H} | \psi \rangle &= \sum_n \left[ E'|C_n|^2 + \epsilon'|C_n|^4 + J'(C_n^* C_{n+1} + C_{n+1}^* C_n) \right. \\
&+ \frac{1}{2} \left( \dot{b}_n^2 + \Omega'(b_{n+1} - b_n)^2 + \frac{1}{2} \mu'(b_{n+1} - b_n)^4 \right) \\
&\left. + \chi'(b_{n+1} - b_n) |C_n|^2 \right],
\end{aligned} \tag{26}$$

where

$$\begin{aligned}
E' &= \frac{E_0}{\hbar\omega}; \quad \epsilon' = \frac{\epsilon}{\hbar\omega}; \quad J' = \frac{J}{\hbar\omega}; \\
\chi' &= \frac{\chi}{\sqrt{\hbar M \omega^3}}; \quad \Omega' = \frac{\Omega}{M \omega^2}; \quad \mu' = \frac{\mu \hbar}{M^2 \omega^3}.
\end{aligned} \tag{27}$$

In order to perform numerical integration of the dynamical equations it is useful to introduce the variables

$$q_n = \frac{C_n + C_n^*}{\sqrt{2}}, \quad p_n = \frac{C_n - C_n^*}{i\sqrt{2}}, \tag{28}$$

so that Eqs.(25) become

$$\dot{q}_n = \left[ E' + \frac{\epsilon'}{2}(q_n^2 + p_n^2) + \chi'(b_{n+1} - b_n) \right] p_n + J'(p_{n+1} + p_{n-1}), \tag{29}$$

$$\dot{p}_n = - \left[ E' + \frac{\epsilon'}{2}(q_n^2 + p_n^2) + \chi'(b_{n+1} - b_n) \right] q_n + J'(q_{n+1} + q_{n-1}), \tag{30}$$

$$\begin{aligned}
\ddot{b}_n &= \Omega'(b_{n+1} - 2b_n + b_{n-1}) + \frac{\chi'}{2} \left( (q_n^2 + p_n^2) - (q_{n-1}^2 + p_{n-1}^2) \right) \\
&+ \mu'[(b_{n+1} - b_n)^3 - (b_n - b_{n-1})^3].
\end{aligned} \tag{31}$$

By denoting with  $\mathcal{B}_n[\mathbf{b}(t), \mathbf{q}(t), \mathbf{p}(t)]$  the r.h.s. of Eq. (31) we have

$$b_n(t + \Delta t) = 2b_n(t) - b_n(t - \Delta t) + (\Delta t)^2 \mathcal{B}_n[\mathbf{b}(t), \mathbf{q}(t), \mathbf{p}(t)] \tag{32}$$

which can be rewritten in the form

$$\begin{aligned}
\dot{b}_n &= \pi_n \\
\dot{\pi}_n &= \mathcal{B}_n[\mathbf{b}(t), \mathbf{q}(t), \mathbf{p}(t)].
\end{aligned} \tag{33}$$

Equations (29) and (30) and the above system have been numerically integrated by combining a finite differences scheme and a leap-frog scheme as follows

$$\begin{aligned}
q_n(t + \Delta t) &= q_n(t) + \Delta t \mathcal{Q}_n[\mathbf{b}(t), \mathbf{q}(t), \mathbf{p}(t)], \\
p_n(t + \Delta t) &= p_n(t) + \Delta t \mathcal{P}_n[\mathbf{b}(t), \mathbf{q}(t), \mathbf{p}(t)], \\
b_n(t + \Delta t) &= b_n(t) + \Delta t \pi_n(t), \\
\pi_n(t + \Delta t) &= \pi_n(t) + \Delta t \mathcal{B}_n[\mathbf{b}(t + \Delta t), \mathbf{q}(t + \Delta t), \mathbf{p}(t + \Delta t)].
\end{aligned} \tag{34}$$

where  $\mathcal{Q}_n[\mathbf{b}(t), \mathbf{q}(t), \mathbf{p}(t)]$  and  $\mathcal{P}_n[\mathbf{b}(t), \mathbf{q}(t), \mathbf{p}(t)]$  are the r.h.s. of Eqs.(29) and (30), respectively. This integration scheme is a symplectic one, meaning that all the Poincaré invariants of a Hamiltonian flow - like the one described by Eqs.(34) - are conserved, among these invariants there is energy. The generating function of the canonical transformation of variables  $\{q_n(t), p_n(t)\} \rightarrow \{q_n(t + \Delta t), p_n(t + \Delta t)\}$  performed by the leap-frog algorithm is explicitly given (thus proving the symplectic character of this algorithm) in Ref.<sup>13</sup>. Therefore energy is well conserved without any drift, just zero-mean fluctuations around a given energy value fixed by the initial conditions. By using sufficiently small time steps  $\Delta t$  any desired precision of energy conservation can be attained.

About the initial conditions, we aim at simulating a physical situation where each photon absorbed by a fluorophore attached to a protein releases - in the average - 0.19 eV of energy to the surrounding electron cloud. This energy is the difference between the energies of the absorbed photon of 4880Å and that of the re-emitted one as fluorescent radiation of 5150Å. We assume, as already stated above, that the effect of a single photon excitation is to make one electron move across the protein by tunnelling through a sequence of potential barriers. In the experiments to which we are referring<sup>1</sup> each protein is labelled with 5-6 fluorochromes, and a laser light is continuously shined on the labelled proteins, therefore what we are after is modelling an elementary process and assuming, in a first approximation, a property of additivity of the same elementary process. In other words, if more than one electron is activated we assume that the resulting physical effect is the sum of a single electron effect. As a consequence, the electron initial condition is assumed to be described by a wavefunction  $C_n(t = 0)$  centered at the site  $n = n_0$  at time  $t = 0$ <sup>14</sup>:

$$C_n(t = 0) = \frac{1}{\sqrt{8\sigma_0}} \text{sech}\left(\frac{n - n_0}{4\sigma_0}\right). \tag{35}$$

where  $\sigma_0 = 3\Omega J/\chi^2$ .

Then, coming to the initial conditions of the phonon component of the system, we assume a thermalized macromolecule at room temperature, that is at  $T = 310K$ . At equilibrium, the energy equipartition theorem for the Hamiltonian (4) reads

$$\left\langle p_n \frac{\partial H_{ph}}{\partial p_n} \right\rangle = \left\langle u_n \frac{\partial H_{ph}}{\partial u_n} \right\rangle = k_B T \tag{36}$$

where  $k_B$  is the Boltzmann constant. At thermal equilibrium, energy is equally shared among all the degrees of freedom and, in particular, between kinetic and potential energies, therefore at  $t = 0$  the velocities and the displacements have been initialized with random values of zero mean and fulfilling the conditions

$$\langle |b_n(0)| \rangle_n = \sqrt{\frac{k_B T}{\hbar \omega \Omega'}}; \quad \langle |\dot{b}_n(0)| \rangle_n = \sqrt{\frac{k_B T}{\hbar \omega}}. \tag{37}$$



Name	Symbol	Value	Symbol	Dimensionless value
Hot-point energy	$E_0$	0.2 eV	$E'$	30
Average mass of amino acids	$M$	$1.5 \times 10^{-25}$ kg	-	-
Spring constant	$\Omega$	18.3 N/m	$\Omega'$	1.2
Electron displacement parameter	$J$	0.0658 eV	$J'$	10
Electron-phonon coupling	$\chi$	61-610 pN	$\chi'$	0.5-5
Anharmonic parameter	$\mu$	Arbitrary	$\mu'$	0-0.5
Nonlinear parameter	$\epsilon$	0.00658-0.0658 eV	$\epsilon'$	1-10

**Table 2.** Values of the parameters used in the numerical simulations. Physical versus dimensionless values are reported.

expressed in dimensionless form. Let us remark that the physical state so modelled consists of a large molecule which is initially at thermal equilibrium, thus the amino-acids constituting the large molecule have random configurations and movements, and then, at some initial time, "hot points" are created on the molecule, bringing it (transiently) out of equilibrium.

In Table 2 the values chosen for the physical parameters are reported. These are: the initial excitation energy  $E_0$ , an average value of the mass  $M$  of the amino acids, the electron displacement parameter  $J$ , the elasticity constant  $\Omega$  used in the numerical studies of Ref.<sup>14</sup>, and the electron-phonon coupling  $\chi$ . In Table 2 also the corresponding dimensionless values of the same physical quantities are reported, these are obtained by using (27) and the frequency  $\omega = 10^{13} \text{s}^{-1}$ .

## Results

All the numerical computations have been performed using an integration time step  $\Delta t = 5 \times 10^{-5}$  entailing a very good energy conservation, with typical relative error  $\Delta E/E \simeq 10^{-5}$ . The length of the chain is  $N = 500$  rounding the number of amino acids of the protein in<sup>1</sup>. Figures (1) and (2) show the spatial distribution of the probability  $|\psi(n, t)|^2$  of finding the moving electron at any site  $n$  versus time for the electron-phonon coupling  $\chi = 100$  pN and  $\chi = 366$  pN, respectively. The electron is initially centered around the site  $n = 250$ . Figure (1) shows that the electron wavefunction quickly spreads over the whole substate of amino acids, a phenomenon somewhat less pronounced in Figure (2) and to some extent counterintuitive since the latter corresponds to a stronger electron-phonon coupling.

Figure (3) shows the time evolution of random initial conditions for the displacements of the underlying chain of masses modelling the chain of amino acids of a protein. The random initial displacements and velocities are generated at thermal equilibrium at 310 K, according to the prescriptions of Eq.(37).

Figure (4) synoptically displays the energy transfer from the electron to the phonon subsystem. The same figure also shows that the larger  $\chi$  the faster this energy transfer, what is physically sound and not necessarily at odds with what reported in Figures (1) and (2) about the electron wavefunction spreading.

As is seen from the plots in Figures (5), the value of the phonon-phonon coupling parameter  $\mu'$  does not seem crucial to control the release of the electron energy to the phonons, the process appears to be mainly driven by the electron-phonon coupling constant. In fact, for  $\chi = 488$  pN the

relaxation to the oscillatory state is quick and practically independent of the value of  $\mu'$ . At the lower value  $\chi = 61$  pN some differences in the relaxation rate are observed by varying  $\mu'$ , but even for  $\mu' = 0$  the energy transfer takes place in both cases of  $\chi = 61$  pN and  $\chi = 488$  pN.

Then we have checked how the phenomenology changes as a consequence of the introduction of the nonlinear coupling in the electron Hamiltonian. In Figures (6) and (7) the effects of different values of the parameter  $\epsilon$  are reported, again for  $\chi = 61$  pN and  $\chi = 488$  pN respectively. Again for  $\chi = 488$  pN the electron energy fastly decrease in time, apart from the case of  $\epsilon = 6.58$  meV where it displays wide oscillations. At  $\chi = 61$  pN the electron energy relaxation is slower and for  $\epsilon = 6.58$  meV it appears to be very slow.

Let us remark that a non-vanishing value of  $\epsilon$ , that is, the presence of the nonlinear coupling term in the electron Hamiltonian, plays a relevant role to ensure a more efficient transfer of part of the electron energy to the phonons of the chain of amino acids.

For any chosen set of physical parameters, except possibly for  $\epsilon = 0$ , the electron always transfers part of its energy to the phonons, and eventually this energy is equally shared among the phonons. In order to work out the typical time scales of this process we have computed the spectral entropy of the normal modes of the chain of amino acids, that is, of the phonons. For the harmonic term  $H_h$  of the dimensionless Hamiltonian (26) we have

$$\langle \psi | \hat{H}_h | \psi \rangle = \frac{1}{2} \sum_{n=1}^N \left[ \dot{b}_n^2 + \Omega' (b_{n+1} - b_n)^2 \right], \quad (38)$$

and then, by following Ref.<sup>13</sup>, the coordinate transformations  $Q_m = S_{mn} b_n$  and  $P_m = S_{mn} \dot{b}_n$ , with

$$S_{mn} = \frac{1}{\sqrt{N}} \left[ \cos\left(\frac{2\pi}{N} mn\right) + \sin\left(\frac{2\pi}{N} mn\right) \right] \quad m, n = 1, 2, \dots, N, \quad (39)$$

transform the Hamiltonian (38) into

$$\tilde{H}_h = \frac{1}{2} \sum_{m=1}^N (P_m^2 + \Omega' \omega_m^2 Q_m^2), \quad (40)$$

where

$$\omega_m^2 = 4 \sin^2\left(\frac{\pi m}{N}\right). \quad (41)$$

Of course, these oscillators are the normal modes (phonons) of the system. Then a spectral entropy  $S(t)$  is defined as

$$S(t) = - \sum_{m=1}^N p_m(t) \ln p_m(t); \quad p_m(t) = \frac{E_m(t)}{E_T(t)} \quad (42)$$

where  $E_T(t) = \sum_{m=1}^N E_m(t)$  and  $E_m(t) = (P_m^2 + \Omega' \omega_m^2 Q_m^2)/2$ , so that the weights  $p_m(t)$  are normalized. The maximum value of  $S(t)$  is attained when all the  $p_m(t)$  are equal to  $1/N$ . Thus, at equipartition, when the energy content of each normal mode is the same, entropy attains its maximum, this allows to define a normalized entropy as

$$\eta(t) = \frac{S_{max}(t) - S(t)}{S_{max}(t) - S(0)}, \quad (43)$$

so that when the phonon oscillators are "frozen" it is  $S(t) = S(0)$  and consequently  $\eta = 1$ ; but at equipartition, when  $S(t) = S_{max}(t)$ , it is  $\eta = 0$ . By following the time decay of  $\eta$ , it is thus possible to find out if and on which time scale the energy released by the electron is definitely transferred to the phonons. In Figure (8)  $\eta(t)$  is plotted as a function of time for various values of the coupling constant  $\chi$  and keeping fixed the other parameters as in the case reported in Figure (1). It is evident that equipartition of energy is always attained, and the time needed for this to happen is rather weakly dependent on the electron-phonon coupling constant. In fact, the decay time is approximately varying between 0.5 ns and 1 ns (the unit time scale being  $10^{-13}$  seconds). Let us remark that the two time scales of the electron energy release to the amino acids and of equipartition of this energy among all the normal modes of the lattice are not equal, and need not to be equal.

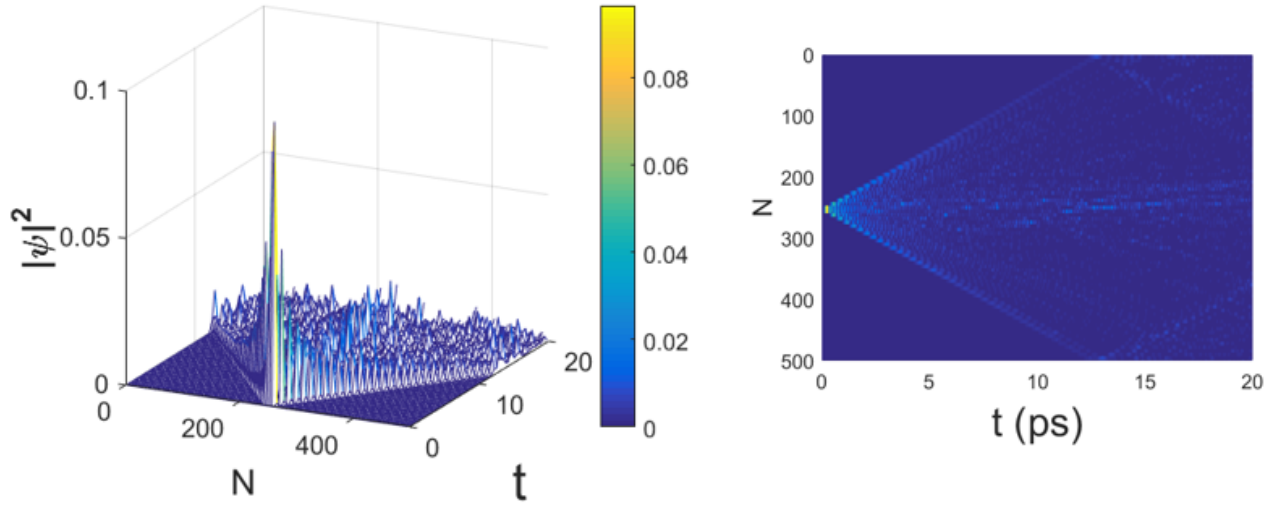


**Figure 1.** (Color online) Evolution of the probability amplitude of an electron  $|\psi(t)|^2$  along the chain of  $N = 500$  amino acids. Initial conditions:  $T = 310^\circ\text{K}$ ,  $E' = 30$ ,  $J' = 10$ ,  $\epsilon' = 5$ ,  $\chi' = 0.8$ ,  $\Omega' = 1.2$ ,  $\mu' = 0.1$ , corresponding to  $E_0 = 0.2$  eV,  $J = 0.0658$  eV,  $\epsilon = 0.0329$  eV,  $\chi = 100$  pN,  $\Omega = 18.3$  N/m, respectively. The right figure is the above view of the left one. Time  $t$  is measured in  $10^{-13}\text{s}$ .

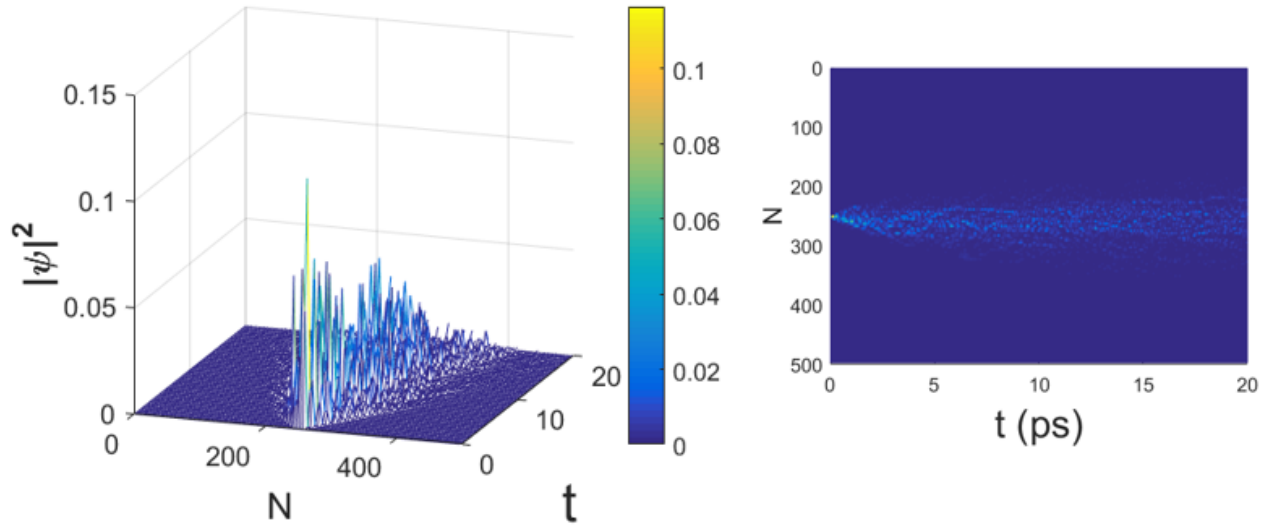


**Figure 2.** (Color online) Evolution of the probability amplitude of an electron  $|\psi(t)|^2$  with  $N = 500$  and  $\chi' = 3$  ( $\chi = 366$  pN); the other parameters are the same of Fig. 1. Time  $t$  is measured in  $10^{-13}$ s.

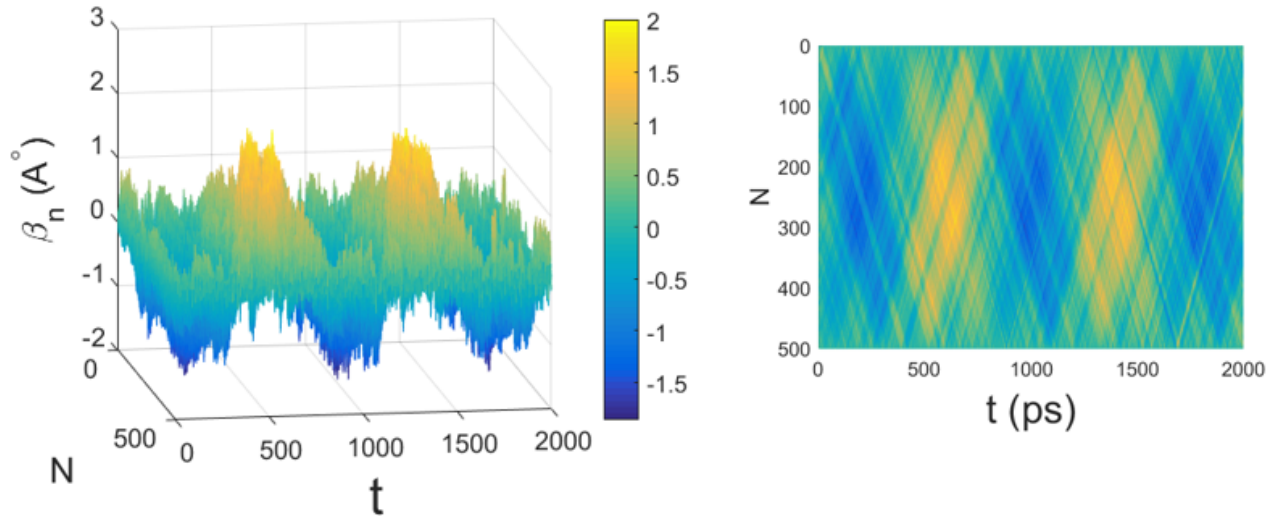


**Figure 3.** (Color online) Time evolution of the average displacements along the chain of  $N = 500$  amino acids. The parameter values are the same of Fig. 1. Time  $t$  is measured in  $10^{-13}$ s.

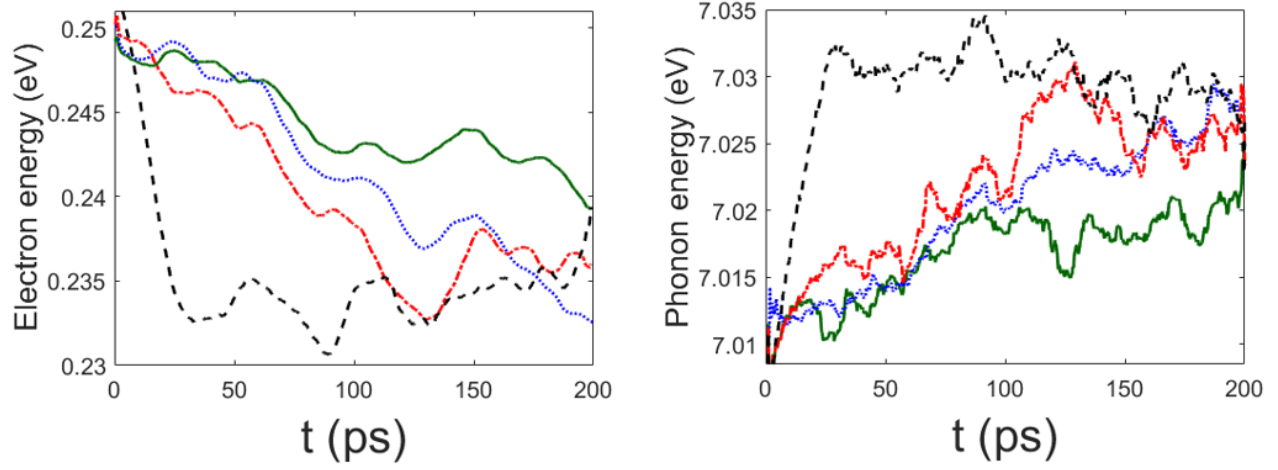


**Figure 4.** (Color online) Energy transfer from the electron to the phonons for  $\chi' = 0.6$  ( $\chi = 73.2$  pN) (green solid line),  $\chi' = 0.8$  ( $\chi = 100$  pN) (blue dotted line),  $\chi' = 1$  ( $\chi = 122$  pN) (red dot-dashed line), and  $\chi' = 1.5$  ( $\chi = 183$  pN) (black dashed line); the other parameters are the same of Fig. 1. Time  $t$  is measured in  $10^{-13}$ s; electron energy and total phonon energy are given in eV.

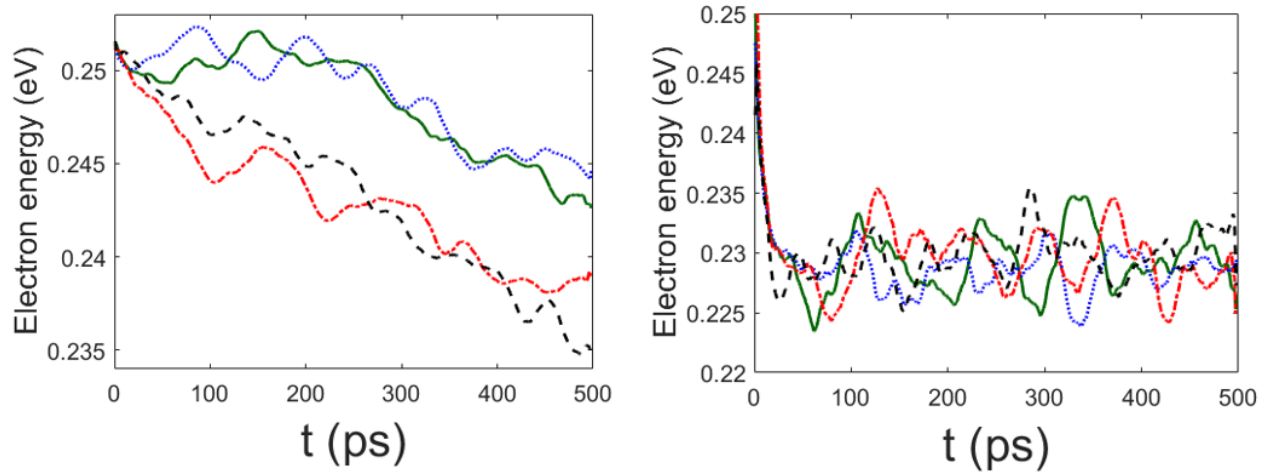


**Figure 5.** (Color online) Decay of the electron energy for  $\mu' = 0$  (green solid line),  $\mu' = 0.1$  (blue dotted line),  $\mu' = 0.3$  (red dot-dashed line), and  $\mu' = 0.5$  (black dashed line); the other parameters are the same of Fig. 1, except for  $\chi' = 0.5$  ( $\chi = 61$  pN) (left panel) and  $\chi' = 4$  ( $\chi = 488$  pN) (right panel). Time  $t$  is measured in  $10^{-13}$ s; electron energy is given in eV.

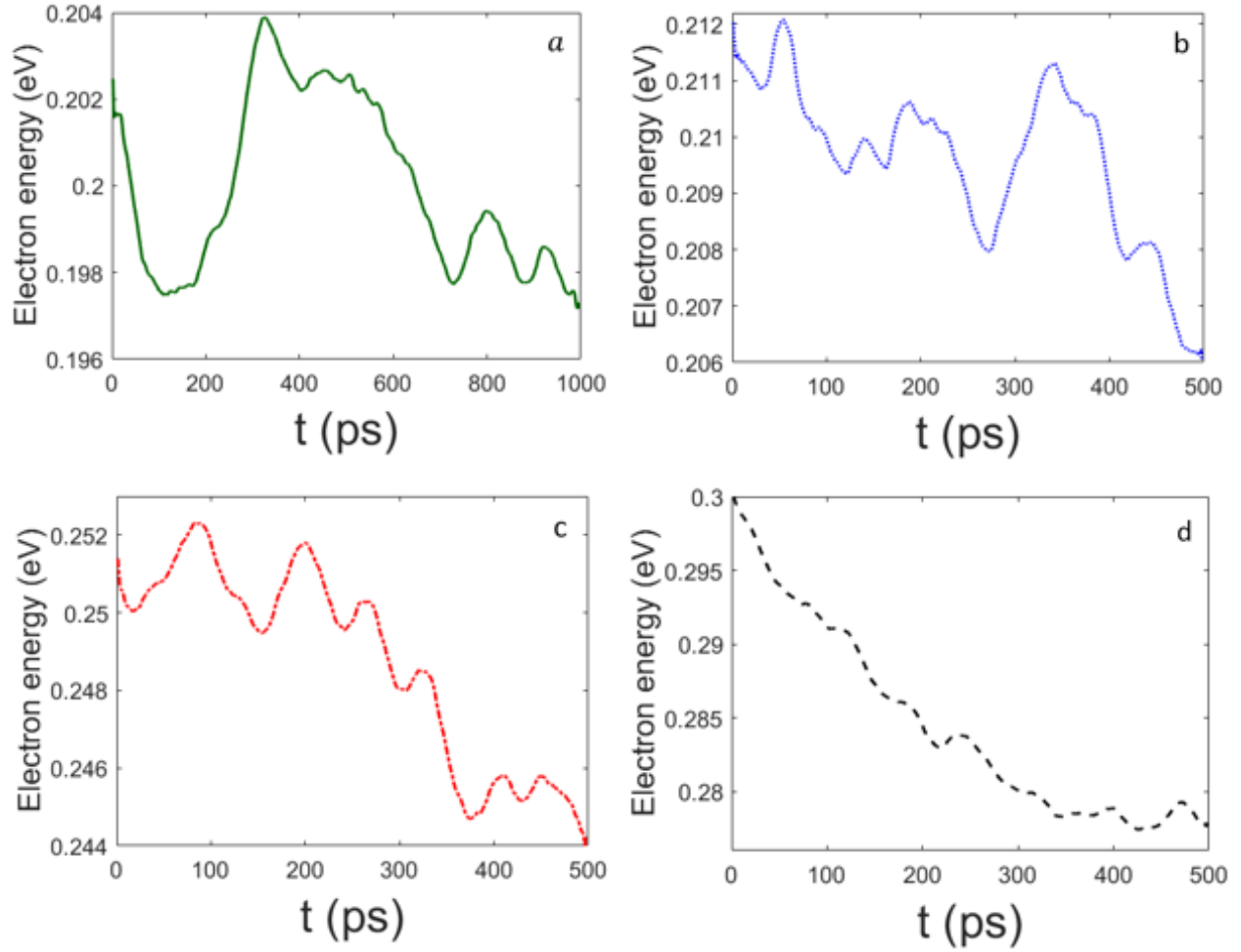


**Figure 6.** (Color online) Decay of the electron energy for a)  $\epsilon = 0$ , b)  $\epsilon' = 1$  ( $\epsilon = 6.58$  meV), c)  $\epsilon' = 5$  ( $\epsilon = 32.9$  meV), and d)  $\epsilon' = 10$  ( $\epsilon = 65.8$  meV); the other parameters are the same of Fig. 1, but  $\chi' = 0.5$  ( $\chi = 61$  pN). Time  $t$  is measured in  $10^{-13}$ s; electron energy is given in eV.

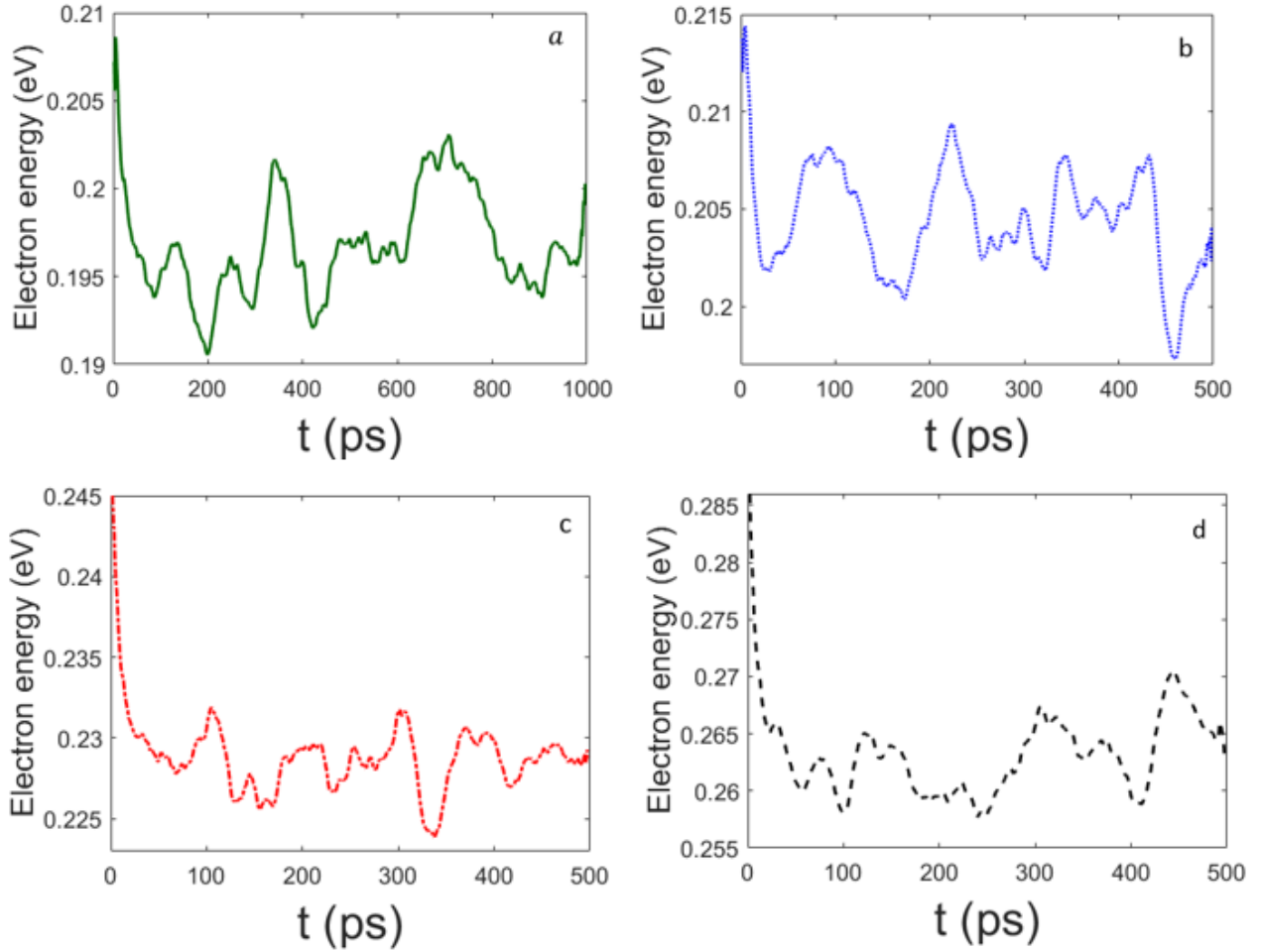


**Figure 7.** (Color online) Decay of the electron energy for a)  $\epsilon = 0$ , b)  $\epsilon' = 1$  ( $\epsilon = 6.58$  meV), c)  $\epsilon' = 5$  ( $\epsilon = 32.9$  meV), and d)  $\epsilon' = 10$  ( $\epsilon = 65.8$  meV); the other parameters are the same of Fig. 1, but  $\chi' = 4$  ( $\chi = 488$  pN). Time  $t$  is measured in  $10^{-13}$ s; electron energy is given in eV.

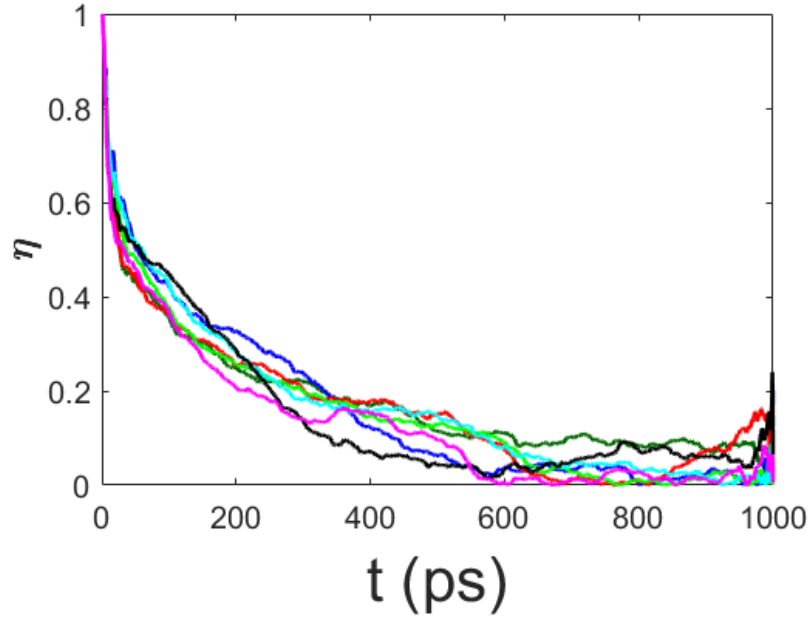


**Figure 8.** (Color online) The spectral entropy  $\eta$  is plotted vs time for  $\chi' = 0.1$  ( $\chi = 12.2$  pN) (dark green),  $\chi' = 0.5$  ( $\chi = 61$  pN) (dark blue),  $\chi' = 1$  ( $\chi = 122$  pN) (red),  $\chi' = 2$  ( $\chi = 244$  pN) (light green),  $\chi' = 3$  ( $\chi = 366$  pN) (light blue),  $\chi' = 4$  ( $\chi = 488$  pN) (black), and  $\chi' = 5$  ( $\chi = 610$  pN) (purple); the other parameters are the same of Fig. 1. Time  $t$  is measured in  $10^{-13}$ s.

## Discussion

Of course we are faced with the problem of understanding what might replace the laser action in living cells. There are several possible candidates to play the role of external energy suppliers, for instance, the hydrolysis of Adenosine Triphosphate (ATP) releases a highly energetic phosphate group, redox reactions and mitochondria produce weak UV photons that might excite Tryptophan and Tyrosine amino acids<sup>9,10</sup> in proteins, as well nucleotides of DNA and RNA. Also an anisotropic momentum transfer operated by water molecules or ions could make the job<sup>11</sup>. In either cases of metabolically generated photons or of ion collisions (phosphate stemming from ATP hydrolysis or other) we can assume that the external energy input for a biomolecule occurs through the generation of "hot points", as in the case of light activated fluorophores, and mediated by either radiative or collisional electronic excitation.

The parameter space of the system investigated here is of course very large, thus we have limited our investigation to a basic choice of physically meaningful parameters with respect to the topic that we aimed at better understanding. Then we have checked the robustness of the phenomenology so observed by changing some parameters, as is the case of the nonlinear coupling constants  $\epsilon$  and  $\mu$ , or the electron-phonon coupling constant  $\chi$ . The results actually show that after having given 0.19eV of initial excitation energy to an electron, the electron wavefunction spreads through the chain by releasing to the phonons only a small fraction of the electron energy, approximately 0.02eV. This is a somewhat unexpected result but interesting because it helps in understanding why exciting a collective intramolecular oscillation of the BSA protein required a very long time. Of course, the contributions of several fluorophores add up, and the continuous illumination of the labelled proteins with an intense laser light allows to accumulate energy in the



protein until the activation threshold of the coherent oscillation of all its atoms is reached and passed over. This implicit assumption of the cumulative character of the fluorophore-contributions comes from the experimental facts observed while working out the results reported in Ref.<sup>1</sup>. We observed that trying to excite the collective vibrations of BSA molecules with different numbers of attached fluorophores, only with at least five attached fluorophores - in the average - the collective vibrations of the BSA molecules were activated. The phonon part has been simplified with respect to the model derived by the de-quantisation of the original Fröhlich's model<sup>4</sup> because the model investigated here has focussed only on the mechanism of down-conversion of the energy of the photons, harvested by the protein through its fluorophores receptors, to the internal vibrations of the chain of amino acids. Although no more than 10% of energy is dissipated by electron to phonons, it seems that in the studied regime no coherent transport of information can occur on the amino acids (as sometimes one could expect in a spin chain model<sup>19</sup>) due to the fact that the electron wave function spreads over all sites. The model studied here can be easily adapted to estimate the efficiency of other excitation mechanisms of biomolecular collective oscillations, like, possibly, the Coulomb collisions of the phosphate anion produced by the hydrolysis of ATP yielding a momentum transfer on some target electron. Or, as already mentioned in the Introduction, by anisotropic momentum transfer operated by water molecules or small ions resulting in collisional excitation of electrons. Let us conclude by mentioning that, for a broad class of Hamiltonian systems, long-living Quasi Stationary States (QSS) can be dynamically generated which keep a system out of thermodynamic equilibrium. Among many other systems where QSS are produced<sup>20</sup>, let us mention a beam of fast particles interacting with the set of waves describing a physical system<sup>21,22</sup>, a situation which is reminiscent, for example, of the above mentioned fast phosphate groups - produced by ATP hydrolysis.

## References

1. I. Nardecchia, J. Torres, M. Lechelon, V. Giliberti, M. Ortolani, P. Nouvel, M. Gori, Y. Meriguet, I. Donato, J. Preto, L. Varani, J. Sturgis, and M. Pettini, *Out-of-Equilibrium Collective Oscillation as Phonon Condensation in a Model Protein*, Phys. Rev. X **8**, 031061 (2018).
2. J. Preto, M. Pettini, and J. A. Tuszynski, *Possible Role of Electrodynamical Interactions in Long-Distance Biomolecular Recognition*, Phys. Rev. E **91**, 052710 (2015).
3. L. Bonetta, *Interactome under construction*, Nature **468**, 851-852 (2010).
4. H. Fröhlich, *Long-range coherence and energy storage in biological systems*, Int. J. Quantum Chem. **2**, 641-649 (1968).
5. Fröhlich, *Selective long range dispersion forces between large systems*, Physics Letters A **39**, 153-154 (1972).
6. Fröhlich, *Long-range coherence in biological systems*, Riv. Nuovo Cimento **7**, 399-418 (1977).
7. I. Nardecchia, L. Spinelli, J. Preto, M. Gori, E. Floriani, S. Jaeger, P. Ferrier, and M. Pettini, *Experimental detection of long-distance interactions between biomolecules through their diffusion behavior: Numerical study*, Phys. Rev. E **90**, 022703 (2014).
8. I. Nardecchia, M. Lechelon, M. Gori, I. Donato, J. Preto, E. Floriani, S. Jaeger, S. Mailfert, D. Marguet, P. Ferrier, and M. Pettini, *Detection of long-range electrostatic interactions between charged molecules by means of fluorescence correlation spectroscopy*, Phys. Rev. E **96**, 022403 (2017).
9. P. Kurian, T.O. Obisesan, and T.J.A. Craddock, *Oxidative species-induced excitonic transport in tubulin aromatic networks: Potential implications for neurodegenerative disease*, J. Photochem. Photobiol. B **175**, 109 -124 (2017) .
10. P. Pospíšil, A. Prasad, M. Rác, *Role of reactive oxygen species in ultra-weak photon emission in biological systems*, J. Photochem. Photobiol. B **139**, 11 (2014).
11. J. P. T. Zaragoza, A. Nguy, N. Minnetian, Z. Deng, A. T. Iavarone, A. R. Offenbacher, and J. P. Klinman, *Detecting and characterizing the kinetic activation of thermal networks in proteins: Thermal transfer from a distal, solvent-exposed loop to the active site in soybean lipoxygenase*, J. Phys. Chem. B **123**, 8662 - 8674 (2019).
12. T. M. Wu and S. Austin, *Bose-Einstein Condensation in Biological Systems*, J. Theor. Biol. **71**, 209 (1978).
13. M. Pettini and M. Landolfi, *Relaxation properties and ergodicity breaking in nonlinear Hamiltonian dynamics*, Phys. Rev. A **41**, 768 (1990).
14. A. Scott, *Davydov's soliton*, Physics Reports **217**, 1 - 67 (1992).
15. H. Fröhlich, *Electrons in lattice fields*, Adv. Phys. **3**, 325 - 361 (1954).
16. T. Holstein, *Studies of polaron motion: Part I. The molecular-crystal model*, Ann. Phys. (USA) **8**, 343 - 389 (1959).
17. I. Cosic, *Macromolecular Bioactivity: Is It Resonant Interaction Between Macromolecules? - Theory and Applications*, IEEE Transact. on Biomed. Engineering **41**,1101 (1994); I. Cosic, *The Resonant Recognition Model of Macromolecular Bioactivity: Theory and Applications*, Birkhauser Verlag, Basel, (1997).

18. V. Veljkovic and I. Slavic, *General model of pseudopotentials*, Phys. Rev. Lett. **29**, 105 - 108 (1972).
19. A. Bayat, D. Burgarth, S. Mancini, and S. Bose, *Memory effects in spin-chain channels for information transmission*, Phys. Rev. **A77**, 050306(R) (2008).
20. A. Campa, T. Dauxois, and S. Ruffo, *Statistical mechanics and dynamics of solvable models with long-range interactions*, Phys. Rep. **480**, 57 (2009).
21. J. Barré, T. Dauxois, G. De Ninno, D. Fanelli, and S. Ruffo, *Statistical theory of high-gain free-electron laser saturation*, Phys. Rev. E **69**, 045501(R) (2004).
22. N. Carlevaro, D. Fanelli, X. Garbet, Ph. Ghendrih, G. Montani, and M. Pettini, *Beam-plasma instability and fast particles: the Lynden-Bell approach*, Plasma Phys. Control. Fusion **56**, 035013 (2014).

## Acknowledgments

E.F. warmly thanks the Fondazione Cassa di Risparmio di Firenze for having co-funded her PhD fellowship. M.P. participated in this work within the framework of the project MOLINT which has received funding from the Excellence Initiative of Aix-Marseille University - A\*Midex, a French “Investissements d’Avenir” programme. R.F. acknowledges support by the QuantERA ERA-NET Co-fund 731473 (Project Q-CLOCKS).

## Author contributions statement

E.F. contributed to the TDVP derivation of the dynamical equations and performed the numerical simulations. R.F. contributed to the TDVP derivation of the dynamical equations. S.M. and M.P. conceived the model and supervised the following activity. All the authors developed the theoretical methods and reviewed the manuscript.

## Additional information

**Competing Interests** The authors declare no competing interests.